Static and Dynamic Vortex Phases in $YBa_2Cu_3O_{7-\delta}$

J. A. Fendrich,* U. Welp, W. K. Kwok, A. E. Koshelev, G. W. Crabtree, and B. W. Veal
Science and Technology Center for Superconductivity & Materials Science Division, Argonne National Laboratory, Argonne, Illinois 60439
(Received 17 May 1996)

Simultaneous magnetization, resistivity, and *I-V* measurements on $YBa_2Cu_3O_{7-\delta}$ show the relationship of the thermodynamic and dynamic behavior near the vortex lattice melting line. We find a coexistence region of solid and liquid at melting, with a first order magnetization jump which is independent of the vortex velocity. Sudden jumps and time dependent hysteresis of the *I-V* curve in the vortex solid phase are interpreted as a relaxation-pinning effect. [S0031-9007(96)01110-6]

PACS numbers: 74.60.Ge, 74.25.Bt, 74.72.Bk

The vortex system in high temperature superconductors is characterized by a vortex liquid phase that covers a large area in the field-temperature plane. For clean systems the transition into the vortex solid phase has been predicted to be first order [1,2], whereas in the presence of pinning induced disorder this transition is believed to be continuous, possibly to a vortex glass [3,4] or Bose glass [5]. For high quality $YBa_2Cu_3O_{7-\delta}$ and $Bi_2Sr_2CaCu_2O_8$ single crystals sharp features in the resistivity [6] and discontinuous jumps in the magnetization [7–11] indicate a first order vortex transition. For both materials it is observed that the vortex melting transition is icelike, that is, the vortex density in the liquid is higher than in the solid.

In addition to these thermodynamic phases, various dynamic vortex phases have been suggested to arise in response to a driving Lorentz force. At least three distinct dynamic phases have been discussed [12]: the moving liquid and the elastically and plastically moving solids. The extent to which dynamic behavior reflects the thermodynamic phase has been widely discussed.

In order to establish the connection between the thermodynamic melting transition and the behavior of the nonthermodynamic transport properties we present simultaneous measurements of the magnetization, resistivity, and *I-V* characteristics of an untwinned $YBa_2Cu_3O_{7-\delta}$ crystal with various applied transport currents. The melting transition is seen as a current independent jump in the magnetization and as the onset of non-Ohmic behavior in the resistivity. On decreasing temperature the onsets of the resistive and magnetic transitions coincide. We observe a first order transition from a moving liquid into a stationary solid at low current densities and into a moving solid at high current densities. A second type of dynamic transition is observed in the vortex solid, characterized by sudden jumps and time dependent hysteresis in the *I–V* curves which imply relaxation processes and stick-slip dynamics. These dynamic transitions do not have any influence on the magnetization.

The sample is an untwinned single crystal of $YBa_2Cu_3O_{7-\delta}$ with dimensions of $1.1 \times 0.7 \times 0.22$ mm^3 and a mass of 1.286 mg. In order to achieve an accurate temperature reading and to avoid comparing results from two different experimental setups the sample was mounted for transport measurements directly onto a thermometer and inserted into the sample space of a SQUID magnetometer. The SQUID voltage and the resistance of the sample were monitored simultaneously while slowly drifting the temperature. During these measurements the sample was held stationary in the center of the SQUID pickup coils.

Figure 1 shows the temperature dependence of the SQUID voltage and of the sample resistivity at low current between 83 and 100 K in an applied field of 4.2 T $\|$ **c**. The SQUID voltage shows the expected variation for

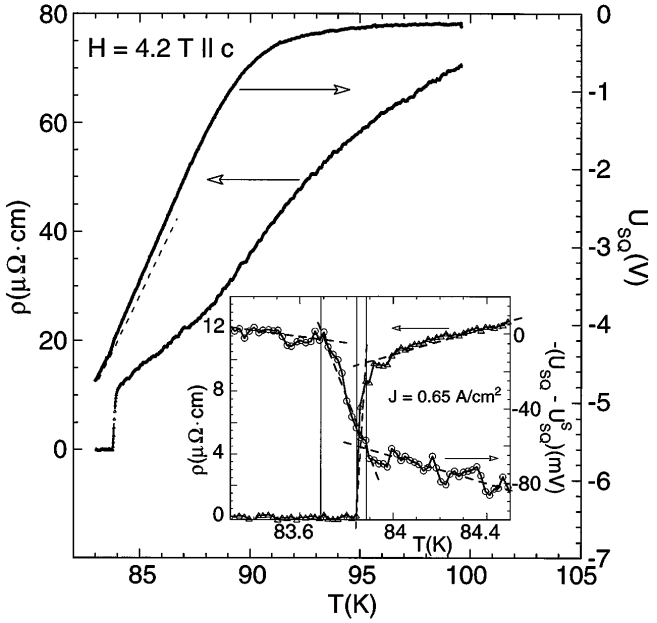

FIG. 1. Simultaneous measurement of the temperature dependence of the SQUID voltage and the sample resistivity. The dotted line represents a linear extrapolation of the low-temperature variation of the SQUID voltage. Inset: Temperature dependence of the SQUID voltage relative to the low-temperature extrapolation and temperature dependence of the resistivity on an expanded temperature scale. The vertical lines mark the onset temperature, zero-resistance temperature, and temperature of completed magnetic transition.

the magnetization: a temperature independent voltage in the normal state and the onset of a sizable diamagnetic signal near the mean-field T_{c2} of about 90 K. Since the baseline of the SQUID voltage is subject to unknown long term drifts, these measurements are not suitable for precise absolute determinations of the magnetization. However, they allow the accurate investigation of sharp relative variations in the magnetization, as occur at the melting transition near 84 K. The inset shows on an expanded temperature scale the variation in the magnetization as reflected in the SQUID voltage, U_{SQ}, with respect to a linear extrapolation of the low temperature variation, U_{SQ}^{S}, which is indicated as a dotted line in the main panel. In order to facilitate the comparison with the resistivity the magnetization data in the inset (and in all following figures) are plotted as $-(U_{\mathrm{SQ}} - U_{\mathrm{SQ}}^{S})$. A distinct jump in the SQUID voltage of about 60 mV is seen consistent with an earlier report [8] on the same crystal. At low current, the onset temperatures T_{on} of the resistive and the magnetic transitions coincide, whereas the completion of the magnetic transition occurs at a much lower temperature, T_f, than the zero resistance temperature, T_z. The magnetic width, $T_{\mathrm{on}} - T_f \approx 200$ mK, is 5 times larger than the resistive width, $T_{\mathrm{on}} - T_z \approx 40$ mK. Similar behavior occurs in a field of 6.5 T [inset of Fig. 2(b)]. Since the slope of the melting line is about 0.5 T/K [8] a temperature width of 200 mK corresponds to a magnetic field width of about 1 kG, too large to be accounted for by geometrical effects or finite demagnetization factors. Instead, we attribute the magnetic width of the vortex melting transition to a spread in transition temperatures caused by chemical inhomogeneities. These inhomogeneities are reflected in the magnetic width (10%–90%) of the superconducting transition at T_c of 0.5 K when measured on warming in 1 G $\|$ **c** after zero-field cooling. We do not believe that pinning is responsible for the width of the magnetic transition, as discussed below.

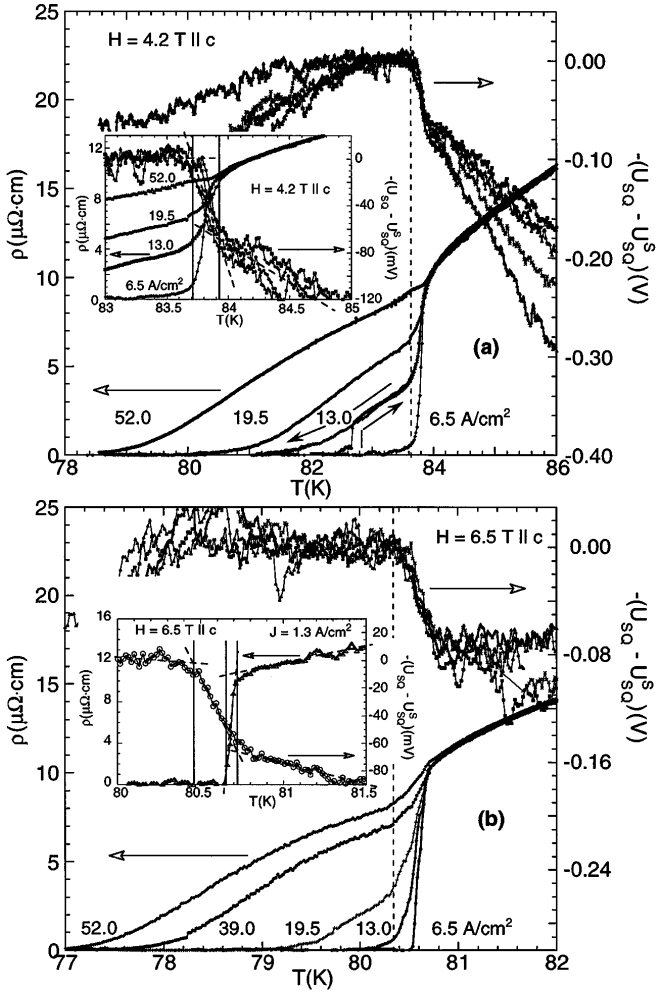

FIG. 2. Temperature dependence of the SQUID voltage plotted as $-(U_{\mathrm{SQ}} - U_{\mathrm{SQ}}^{S})$ and of the resistivity at various transport current densities in an applied field of 4.2 T $\|$ **c** (upper panel) and 6.5 T $\|$ **c** (lower panel). The insets show the transitions on expanded temperature scales.

The variation of the magnetization reflects the fraction of solidified vortices: it is zero at temperatures above T_{on} and unity at temperatures below T_f. In the transition region between T_{on} and T_f a two-phase region of coexisting liquid and solid is realized. This progression of solidification allows for an interpretation of the transport behavior. At low current densities the resistivity goes to zero within the coexistence region at a solid/liquid ratio which for the data in Fig. 1 is 20% solid/80% liquid. This is suggestive of the percolative development of a superconducting path across the sample [13], which would occur at 16% in a three dimensional system.

The behavior at high current densities is shown in the main panels of Fig. 2 for applied fields of 4.2 and 6.5 T, respectively. For these measurements the magnetic field has been applied at temperatures above the melting transition. Data were taken subsequently on cooling and warming. The resistive transitions show the familiar non-Ohmic broadening, and zero resistance occurs at temperatures below the coexistence region. This indicates a transition at melting from a moving liquid into a moving solid. At the highest current densities the resistive transition is almost fully suppressed and the resistivity has nearly reached the level of the liquid state. In contrast, the magnetic transition does not change with current density as shown in the inset of the top panel on an expanded scale. The transition temperature and transition width are current independent to within 50 mK, and the jump height is constant within 15% implying that at low and high current densities the same thermodynamic transition occurs involving the same number of vortices. The thermodynamic melting transition in our relatively clean sample is not affected by the motion of the vortex system.

The resistive transition at high current shows new features which can be interpreted with the magnetic data. The temperature dependence of the resistivity can be divided into three regimes: a weak dependence in the vortex liquid state, a steep decrease in the transition region, and a weak dependence in the solid phase that

gradually approaches zero. As indicated by the dotted lines in Fig. 2 the resistive transition region coincides with the coexistence region in the magnetic transition. This suggests that the steep temperature dependence of the resistivity is a manifestation of the rapid growth of the vortex solid phase which is pinned more effectively through its finite shear modulus than is the liquid. Once solidification is completed near T_f the temperature dependence of the resistivity crosses over to that of the moving solid. The offset in the resistivities between the liquid and solid phases is a measure of the enhanced pinning in the vortex solid. At high current the offset resistivity is nearly reduced to zero indicating that pinning is effectively eliminated from the moving vortex solid, consistent with neutron diffraction experiments on other materials [14] and with general theoretical expectations [12]. Therefore, the magnetization data at high current reflect the intrinsic behavior in the absence of pinning. The current independence of the width and the height of the magnetic jump shows that pinning which is active at low current is not strong enough in our relatively clean sample to alter the thermodynamic transition at melting.

A sharp hysteresis in the temperature dependence of the resistivity between warming and cooling at 13 A/cm^2 in a field of 4.2 T indicates a second type of dynamic transition in the vortex solid. On cooling the resistivity approaches zero smoothly, whereas on warming the resistivity stays zero to higher temperatures followed by a slight increase to a small nonzero value and then a jump up to the cooling curve. This hysteresis does not appear when the temperature is increased before the sample resistance has reached zero. Similar hysteretic effects have been reported in the transport properties of low-T_c materials [15] and have generally been associated with plastic motion of the slowly moving vortex solid. Resistive hysteresis has been observed at the thermodynamic melting transition between the vortex liquid and solid phase [6]. For the present sample at 84 K, 4.2 T, and at a current density of 0.065 A/cm^2 hysteresis at the melting transition is less than 30 G in magnetic field corresponding to a hysteresis in temperature too small to be discernible in the data of Figs. 1 and 2. The hysteresis at melting is readily suppressed with increasing current. In contrast, the hysteresis discussed here occurs at the dynamic transition from a stationary to a moving vortex solid at temperatures well below melting. It is more pronounced at higher currents that are strong enough to dislodge the vortex solid.

The hysteretic effects can be studied in more detail at fixed temperatures and fixed field using *I-V* characteristics as shown in Fig. 3(a). The *I-V* characteristics consist of two branches, a static branch at zero voltage and a dynamic branch following the traditional smooth non-Ohmic *I-V* behavior. For currents increasing from zero we observe a sharp jump of the voltage from the static branch to the dynamic branch at a critical current I_c. This jump occurs at higher values of I_c as the temperature is decreased. At currents above I_c the *I-V* curve is

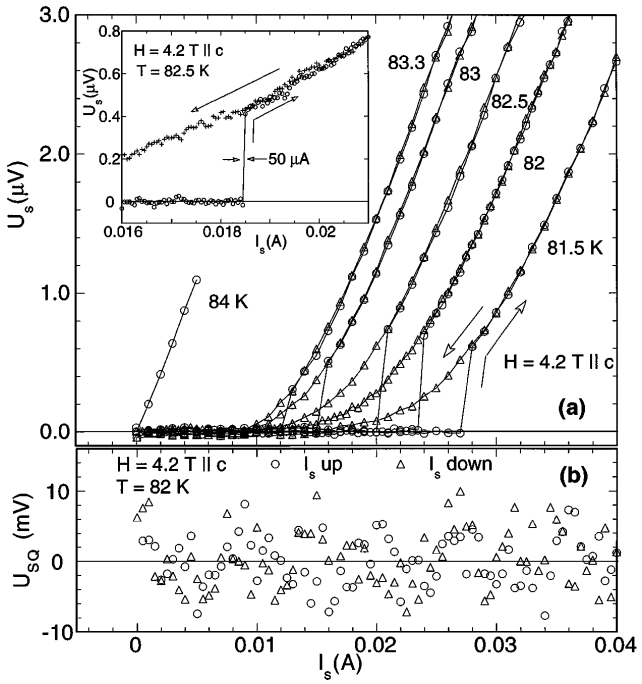

FIG. 3. Upper panel: *I-V* characteristics taken at various temperatures for increasing and decreasing dc currents as indicated by the arrows. The inset shows the sharpness of the jump in the voltage when measured with current increments of 50 μA. Lower panel: Current dependence of the magnetization for increasing (○) and decreasing (△) current. The SQUID voltage has been corrected for a monotonic background caused by the baseline drifts and by the magnetic moment created by the applied current.

reversible, whereas for currents below I_c the dynamic branch describes decreasing current and the static branch increasing current. The realization of these states depends on history. The voltage jumps occur into a fairly rapidly moving state with an average velocity about 10% of that in the liquid state. The jumps in the *I-V* curves are sharp without any structure or intermediate points as can be seen in the inset to Fig. 3. The current dependence [Fig. 3(b)] as well as the temperature dependence [Fig. 2(a)] of the magnetization show that there is no magnetization feature within our resolution of 10 mV that correlates with the voltage jumps. This is consistent with our interpretation of the voltage jumps as reflecting dynamic behavior in the solid phase.

As mentioned above, the hysteretic behavior occurs only if the sample has been at zero voltage, that is, in a pinned vortex state. In fact, the critical current increases with the time the system was held at zero current as shown in Fig. 4. This aging process can be understood as relaxation of the vortex system into lower energy metastable pinning states with time [16]. Elastic and plastic deformations of the vortex system at rest allow it to relax locally into deeper pinning potential wells, increasing the critical current necessary to depin the system. By this aging process the vortex system traps itself. The time spent at rest determines the typical barrier

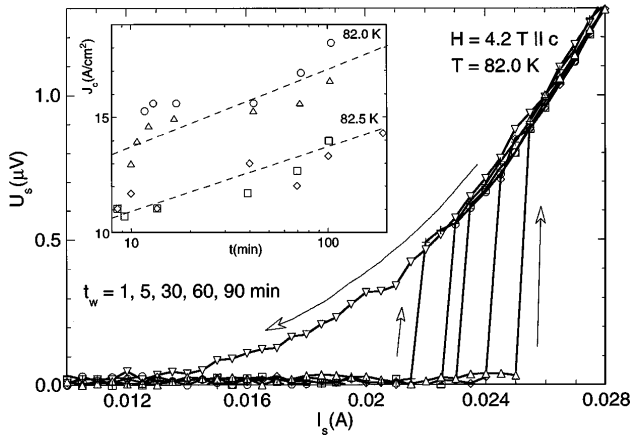

FIG. 4. Time dependence of the *I-V* characteristics. t_w denotes the time the system was held at zero current. The inset shows the time dependence of the critical current density for two data sets at 82.0 and at 82.5 K, respectively. Here, the time t is the sum of t_w and the time taken to ramp the current to its critical value.

height U_t the system can overcome during the relaxation process according to $U_t = k_B T \ln(t/t_0)$, where t_0 is an attempt time. Thus, the critical current after aging should increase monotonously with aging time, as is shown in the inset of Fig. 4. In our experiment the current is increased continuously from zero after aging, so that current induced relaxation effects occurring between zero and the critical current will contribute to the critical current in addition to the time dependence of the barrier height.

The observed behavior is reminiscent of processes involving dynamic and static friction. A perturbation in a system at the static limit, for example, a sand pile that is inclined, induces avalanches that establish a new steady state determined by dynamic friction. The vortex system at currents just below I_c is at the static limit, held by the highest barriers attained in the aging process. Just above I_c there are no barriers or dynamic states corresponding to small velocities (those occur at small currents on the decreasing branch of the *I-V* curve). The vortex system depins suddenly and its velocity jumps to the value corresponding to the imposed current and to dynamic friction. The sharpness of the jumps and the absence of any intermediate structure suggests that the entire vortex system depins as a whole and starts to move coherently.

In this model a balance between elastic energy and pinning energy is crucial for the occurrence of the aging process. If pinning is too weak or elastic energies are too high, the necessary relaxation processes are unlikely to occur preventing the establishment of static friction that is significantly larger than dynamic friction.

In conclusion, simultaneous measurements of the resistivity and magnetization reveal the relationship between the thermodynamic and dynamic behavior near the vortex lattice melting line of $YBa_2Cu_3O_{7-\delta}$. The melting transition is seen as a current independent jump in the magnetization and as the onset of non-Ohmic behavior in the resistivity. The onsets (on decreasing temperature) of the magnetic and resistive transitions coincide, and the width of the magnetic transition marks a coexistence region of vortex solid and vortex liquid. Time dependent and hysteretic jumps in the *I-V* curves in the vortex solid state indicate relaxation processes and slip-stick dynamics.

Work supported by the NSF Science and Technology Center for Superconductivity under Contract No. DMR 91-20000 (J.A.F., A.E.K.) and the DOE Basic Energy Science-Material Science under Contract No. W-31-109-ENG-38 (U.W., W.K.K., G.W.C., B.V.).

*Present address: 313 Microelectronics, University of Illinois, 208 N. Wright Street, Urbana, IL 61801

[1] E. Brezin *et al.,* Phys. Rev. B **31**, 7124 (1985).
[2] D. R. Nelson *et al.,* Phys. Rev. Lett. **60**, 1973 (1988).
[3] M. P. A. Fisher, Phys. Rev. Lett. **62**, 1415 (1989).
[4] D. S. Fisher *et al.,* Phys. Rev. B **43**, 130 (1991).
[5] D. R. Nelson and V. M. Vinokur, Phys. Rev. Lett. **68**, 2398 (1992); Phys. Rev. B **48**, 13 060 (1993).
[6] H. Safar *et al.,* Phys. Rev. Lett. **69**, 824 (1992); **70**, 3800 (1993); W. K. Kwok *et al.,* Phys. Rev. Lett. **69**, 3370 (1992); **72**, 1088 (1994); M. Charalambous *et al.,* Phys. Rev. Lett. **71**, 436 (1993); J. A. Fendrich *et al.,* Phys. Rev. Lett. **74**, 1210 (1995); S. Watauchi *et al.,* Physica (Amsterdam) **259C**, 373 (1996); K. Kadowaki *et al.,* Physica (Amsterdam) **263C**, 164 (1996).
[7] R. Liang *et al.,* Phys. Rev. Lett. **76**, 835 (1996).
[8] U. Welp *et al.,* Phys. Rev. Lett. **76**, 4809 (1996).
[9] H. Pastoriza *et al.,* Phys. Rev. Lett. **72**, 2951 (1994).
[10] E. Zeldov *et al.,* Nature (London) **375**, 373 (1995).
[11] B. Revaz *et al.,* Europhys. Lett. **33**, 701 (1996); T. Hanaguri *et al.,* Physica (Amsterdam) **256C**, 111 (1996).
[12] H. J. Jensen *et al.,* J. Low Temp. Phys. **74**, 293 (1989); A. C. Shi and A. J. Berlinskii, Phys. Rev. Lett. **67**, 1926 (1991); A. E. Koshelev, Physica (Amsterdam) **198C**, 371 (1992); A. E. Koshelev and V. M. Vinokur, Phys. Rev. Lett. **73**, 3580 (1994); F. Nori, Science **271**, 1373 (1996); N. Gronbech-Jensen *et al.,* Phys. Rev. Lett. **76**, 2985 (1996); T. Giamarchi and P. Le Doussal, Phys. Rev. Lett. **76**, 3408 (1996).
[13] G. Deutcher, in *Percolation, Localization and Superconductivity,* NATO Advanced Study Institutes (Plenum Press, New York, 1984), p. 94.
[14] P. Thorel *et al.,* J. Phys. (Paris) **34**, 447 (1973); U. Yaron *et al.,* Nature (London) **376**, 753 (1995).
[15] R. Wördenweber and P. H. Kes, Phys. Rev. B **33**, 3172 (1986); **34**, 494 (1986); S. Bhattacharya and M. J. Higgins, *ibid.* **52**, 64 (1995); M. J. Higgins and S. Bhattacharya, Physica (Amsterdam) **257C**, 232 (1996).
[16] V. B. Geshkenbein *et al.,* Phys. Rev. B **48**, 9917 (1993).